

Synergistic Interactions of Sugars/Polyols and Monovalent Salts with Phospholipids Depend upon Sugar/Polyol Complexity and Anion Identity

Ginevra A. Clark,[†] J. Michael Henderson,[†] Charles Heffern,[†] Bülent Akgün,^{‡,§,||} Jaroslaw Majewski,^{⊥,#} and Ka Yee C. Lee^{*,†}

[†]Department of Chemistry, Institute for Biophysical Dynamics, James Franck Institute, The University of Chicago, Chicago, Illinois 60637, United States

[‡]Department of Chemistry, Bogazici University, Bebek, Istanbul 34342, Turkey

[§]National Institute of Standards and Technology, Gaithersburg, Maryland 20899-6102, United States

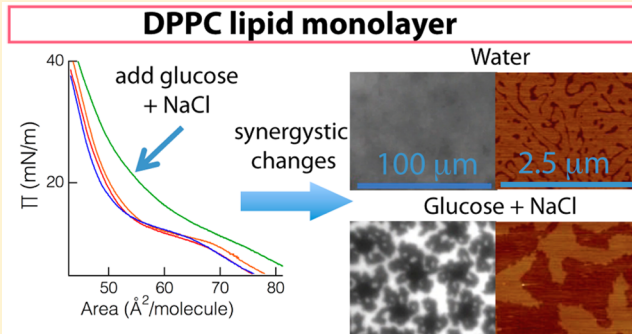
^{||}Department of Materials Science and Engineering, University of Maryland, College Park, Maryland 20742, United States

[⊥]Los Alamos Neutron Scattering Center/MPA/CINT, Los Alamos National Laboratory, Los Alamos, New Mexico 87545, United States

[#]Department of Chemical Engineering, University of California, Davis, California 95616, United States

Supporting Information

ABSTRACT: We found that interactions of dipalmitoylphosphatidylcholine (DPPC) lipid monolayers with sugars are influenced by addition of NaCl. This work is of general importance in understanding how sugar–lipid–salt interactions impact biological systems. Using Langmuir isothermal compressions, fluorescence microscopy, atomic force microscopy, and neutron reflectometry, we examined DPPC monolayers upon addition of sugars/polyols and/or monovalent salts. Sugar–lipid interactions in the presence of NaCl increased with increasing complexity of the sugar/polyol in the order glycerol ≪ glucose < trehalose. When the anion was altered in the series NaF, NaCl, and NaBr, only minor differences were observed. When comparing LiCl, NaCl, and KCl, sodium chloride had the greatest influence on glucose and trehalose interactions with DPPC. We propose that heterogeneity created by cation binding allows for sugars to bind the lipid headgroups. While cation binding increases in the order $K^+ < Na^+ < Li^+$, lithium ions may also compete with glucose for binding sites. Thus, both cooperative and competitive factors contribute to the overall influence of salts on sugar–lipid interactions.



■ INTRODUCTION

During a normal breathing cycle, lung surfactant, a mixture of lipids and proteins that coats the alveolar surface, undergoes a series of phase and morphological changes in response to the rapid changes in alveoli surface area.¹ A thorough understanding of these changes is critical for a mechanistic understanding of lung surfactant under both the normal and diseased states. Langmuir monolayers have been successfully used as model systems for lung surfactant and have revealed the mechanisms for the proper functioning of the lung.² Recently we have examined the behavior of lung surfactant at high surface pressure to elucidate the modes of collapse that lung surfactant undergoes at the end of exhalation. When glycerol is present in the subphase, larger scale folding of the lipid monolayer is observed. This intriguing finding points to the possibility that the presence of glycerol increases the stiffness of the monolayer and raises questions as to how polyols interact

with lipids, how these interactions might differ from one polyol to another, and how they might affect the phase behavior of lipid films.

As the fields of tissue engineering, cell transplantation, and stem cell biology grow, there is an emerging need for well-preserved tissue samples from many sources.³ Sugars, including glucose and trehalose, are known to have cryoprotective properties, but the mechanisms by which they offer protection remain poorly understood.^{4,5} Improvements in the preservation of organs for transplant would no doubt improve patient outcomes.⁶ Recent studies using rat livers demonstrated that a glucose derivative (3-O-methyl-D-glucose) has significant preservative properties⁶ at concentrations similar to the glucose

Received: August 4, 2015

Revised: October 7, 2015

Published: October 23, 2015



concentrations used in this study. The strategy of *ex vivo* lung perfusion (EVLP) has recently been developed to restore donor lungs under normothermic conditions in a solution containing dextrose.⁷ EVLP treatment rendered damaged donor lungs suitable for transplant, with positive patient outcomes. Further, it is known that glucose is depleted in the alveolar lining^{8,9} and that diabetes leads to diminished lung compliance.^{10,11} These studies illustrate the need to understand the interaction of sugars with membranes under different conditions (i.e., monolayers, bilayers, and low or high temperatures) in order to make advances in tissue preservation and to better understand disease.

Despite decades of research efforts, the importance of sugar-lipid interactions in cryoprotection is poorly understood.^{12–14} While numerous studies have demonstrated a depletion of sugars near lipid membrane surfaces,^{5,14–16} specific sugar-lipid interactions have been identified, experimentally^{4,12,17} and *in silico*.^{18,19} Our work supports the more nuanced views of sugar-lipid interactions that have recently emerged and are supported by both experimental results and molecular dynamics simulations.^{20,21} These studies propose that sugars are enriched at the surface at low concentrations and depleted from the surface at high concentrations. In the context of understanding cryoprotection, our results contribute to a larger conversation that is helping to bridge conflicting views on how cryoprotectants interact with membranes and offer protection.^{22,23} Namely, a mechanism that not only includes specific membrane-cryoprotectant interactions but also water-cryoprotectant interactions is emerging. Most modern studies have been performed with bilayers, where research has centered on the protective properties of sugars during freeze-drying.²⁴ Here, we sought to improve current understanding of sugar-lipid interactions by examining monolayers, which allow for facile comparison of many system components, imaging, and control of surface pressure. In this work, we examined how glycerol, glucose, and trehalose interact with dipalmitoylphosphatidylcholine (DPPC) monolayers in the presence or absence of various salts. Different salt conditions provided a route for us to perturb sugar-lipid interactions, giving us a better view of the subtleties involved in these interactions, and providing insights at physiologically relevant conditions.

This study is of general significance in elucidating the effects of salts on the interactions of lipids with other molecules. While many studies have considered independently the effects of sugars or salts on lipid monolayers and bilayers, few studies have examined the cooperative/competitive effects of multiple binding partners.^{25–29} The Hofmeister series, a series of salts in which the charge density of the anion or cation is varied with the purpose of influencing solution properties, is known to differentially influence protein-protein interactions, protein-DNA interactions, and lipid packing in monolayers and bilayers.^{30–32} However, to the best of our knowledge, there are no studies in the literature examining how a kosmotropic/chaotropic series impacts zwitterionic lipid interactions with sugars or other small molecules. Our examination of the Hofmeister series here allows us to see the independent role the anion or cation plays in perturbing lipid interactions with other molecules.

In this study, we used a multipronged approach to elucidate the interactions of sugars or polyols with monovalent salts and DPPC. Full characterization of the system of interest was performed using a combination of isotherm measurements, fluorescence microscopy (FM), atomic force microscopy

(AFM), and neutron reflectivity (NR). The former two allowed us to examine morphological changes occurring in the monolayer in the presence of sugars and/or salts as the surface pressure is varied.³³ Changes in domain size and shape provide clues as to how sugars interact with the monolayer under different salt conditions.^{34,35} AFM, on the other hand, makes it possible for us to image the monolayer at higher magnification, allowing us to resolve fine features that are not accessible via optical microscopy. Finally, NR provides information on the structure in the direction perpendicular to the monolayer and allowed us to deduce distributions of sugar species at the interface.² By extending the study to include different combinations of sugar (glycerol, glucose, trehalose) and ion (Li^+ , Na^+ , K^+ , F^- , Cl^- , Br^-), we are also able to determine the role of sugar structure, anion, and cation in the observed morphological changes. With this information in hand, we are in a position to develop a clear understanding of the cooperative and competitive factors that can influence sugar and salt interactions with a zwitterionic lipid.

■ EXPERIMENTAL SECTION

Materials. All materials were obtained in high purity and used without further purification. 1,2-Dipalmitoylphosphatidylcholine (DPPC) was obtained as a powder from Avanti Polar Lipids (Alabaster, AL). The fluorescence probe used for visualization was Texas-Red-labeled 1,2-dihexadecanoyl-sn-glycerol-3-phosphoethanolamine (TR-DHPE) obtained from Molecular Probes (Eugene, OR). The lipids were dissolved in chloroform (HPLC grade, Fischer Scientific, Pittsburgh, PA) to make stock solutions at the concentration specified. All of the sugars and salts were obtained from Sigma-Aldrich (St. Louis, MO) in the following purities: sodium fluoride (Acros, 99+ % for analysis), sodium bromide (Acros, 99.5%, for analysis), sodium chloride (Acros, extra pure), potassium chloride (Acros, extra pure), lithium chloride (Alfa Aesar, 99.9%), glycerol (Sigma, spectrophotometric grade), D-(+)-glucose (Sigma BioUltra), and D-(+)-trehalose dihydrate (Fluka Analytical). Water used in experiments was purified through a Milli-Q system (Millipore, Billerica, MA) with a resistivity of >18 MΩ·cm. D₂O for neutron reflectivity experiments was obtained from Sigma-Aldrich.

Langmuir Isotherm and Fluorescence Microscopy (FM). The Langmuir trough setup has been described previously.^{33,36} Briefly, it consists of a home-built Teflon trough with two moveable Teflon barriers whose motions are precisely controlled by a pair of translational stages (UTM100, Newport, Irvine, CA) for symmetric compression of monolayers at the air/water interface. A stationary Wilhelmy balance (Riegler and Kirstein, Berlin, Germany) is used to measure surface pressure. As the surface area is reduced, the change in surface pressure, defined as the difference in surface tension between a pure air/liquid interface and one with an adsorbed monolayer, is monitored.

The subphase temperature is maintained within 0.5 °C of the desired temperature with a home-built temperature control station composed of thermoelectric units (Marlow Industries, Dallas, TX) joined to a heat sink held at 20 °C by a Neslab RTE-100 water circulator (Portsmouth, NH). A piece of resistively heated coverglass (Delta Technologies, Dallas, TX) is placed above the sample to suppress evaporative losses, minimize convective currents, and prevent condensation of water on the microscope objective.

The trough assembly is fixed to a custom-built microscope stage to allow for simultaneous imaging by FM with a 50× ELWD objective (Nikon Y-FL, Fryer, Hertley, IL). A high-pressure mercury lamp (Osram Company, Sylvania, Danvers, MA) is used for fluorescence excitation, and the emitted light was gathered with a dichroic/mirror filter cube (Nikon HYQ Texas Red, Fryer, Hertley, IL). Images from the fluorescence microscope are collected at a rate of 30 frames/s using a CCD camera (Stanford Photonics, Palo Alto, CA) and recorded on a Sony digital videocassette recorder (Sony B&H Photo-

Video, New York, NY). This assembly permits monolayer morphology to be observed over a large lateral area while isotherm data are obtained. The entire assembly is mounted on a vibration isolation table (Newport, Irvine, CA) and controlled by custom software written using Lab View 6.1 (National Instruments, Dallas, TX).

All experiments were performed at 25 °C using Milli-Q water. Each 80 mL subphase was composed of pure water, with specified w/v % sugar (glycerol, glucose, or trehalose) and/or specified concentration (mM) of salt (NaF, NaCl, NaBr, LiCl, or KCl). The surface balance was calibrated to the value of the surface tension of pure water at 25 °C. The lipids were dissolved in chloroform at a final concentration of 0.1 mg/mL, with 99 mol % DPPC and 1 mol % TR-DHPE. The lipid solution was spread onto the appropriate subphase by dropwise addition and allowed to stand for 15 min to ensure evaporation of organic solvent. The barriers were compressed at a linear speed of 0.1 mm s⁻¹ (6.35 mm² s⁻¹), and isotherm data in the form of surface pressure Π (mN m⁻¹) versus area per lipid molecule (Å² molecule⁻¹) were collected at 1 s intervals until the compression limit was reached. The surface morphology was monitored continuously via FM throughout the compression. Contrast was obtained by the inclusion of TR-DHPE, which preferentially partitions into the more fluid phase of the monolayer. Thus, the fluid phase was rendered bright while the condensed phase remained dark.

Atomic Force Microscopy. Higher resolution imaging of the monolayer was obtained via AFM imaging. After compressing the monolayer in the Langmuir trough to the desired surface pressure of 30 mN m⁻¹ at 25 °C, the film was transferred from the air/water interface onto a mica substrate (Ted Pella, Inc. Redding, CA) by the inverse Langmuir–Schaefer transfer technique, as previously described.³³ Briefly, the mica substrate was placed on a stainless steel apparatus with a surrounding 2 mm high machined knife edge, and the entire setup was placed at the bottom of the trough where it remained submerged in the subphase throughout the compression. At the desired surface pressure, the subphase was slowly aspirated from the trough to lower the subphase level and the knife edge eventually cut the monolayer as the surface height lowered, preserving the monolayer at the desired surface pressure. Drilled holes in the bottom of the steel piece allowed water to exit the chamber completely until the monolayer was deposited on the mica substrate. Transfer was conducted at 30 mN/m to ensure a film stiff enough that the integrity of the film was preserved during the transfer process; monolayer morphology before, during, and after transfer was monitored to ensure that the surface morphology was not perturbed. Lipid monolayers transferred to mica substrates were imaged at ambient temperature in air using a Multimode Nanoscope IIIA scanning probe microscope (Digital Instruments, Santa Barbara, CA) with a Type J scanner in contact mode. Silicon nitride tips NP-S (AFM Bruker Probes, Camarillo, CA) with a nominal spring constant of 0.32 N/m were used. The surface of the tips were decontaminated by UV-generated ozone before sampling (PSD-UV Surface Decontamination System, Novascan, Ames, IA).³⁷

Neutron Reflectometry. Neutron reflectometry (NR) was used to obtain the scattering length density ($\beta(z)$) distribution perpendicular to the monolayer surface. Analysis of $\beta(z)$ provides information on the surface averaged distribution of lipids and small molecules in the “z” direction. Neutron scattering contrast is obtained due to the fact that neutrons reflect differently off different nuclei. As hydrogen and deuterium have very different neutron scattering cross sections, contrast can be enhanced by the judicious deuteration of lipids and subphase components.

NR measurements on monolayers at the air/liquid interface were performed at the NG-7 horizontal neutron reflectometer at NIST Center for Neutron Research (Gaithersburg, MD) with an incident neutron wavelength of 4.75 Å. A Langmuir trough with a Wilhelmy plate and moveable barrier was mounted to the reflectometer. The incident angle of the neutron beam was varied to obtain scattered neutron intensity distribution as a function of the momentum transfer vector Q_z ($Q_z = 4\pi \sin(\theta)/\lambda$, where θ is the incident angle of the neutron beam and λ is the wavelength of the neutrons), varying from 0.01 to 0.24 Å⁻¹.

Monolayers of DPPC-d75 (deuterated headgroups and tails; see Figure 5A) were spread at a surface pressure of ~8 mN/m, allowed to equilibrate for 1 h, and compressed to 20 mN/m at room temperature (23 °C). The subphase was composed of D₂O, with varying amounts of glucose (0, 2.5, or 5 w/v % glucose) and concentrations of NaCl (0, 100, and 200 mM). Such isotopic construction of the arrangement (partially deuterated lipid monolayer–hydrogenated glucose–D₂O subphase) provides the best contrast conditions to observe even minute changes in the structure of the investigated systems. Fitting of the scattering data is done using the Paratt formalism: a model-dependent fitting algorithm in Motofit where the components of the investigated system (along the z-direction) are described by slabs of constant $\beta(z)$ and interconnected by error function to represent roughness.³⁸

RESULTS

Isothermal Compressions of DPPC Monolayers with NaCl and Sugars. Isotherms provide information about the phase behavior of the monolayer as a function of lipid packing density. When spread at full expansion of the trough, the lipid molecules are in a gas (G)–liquid-expanded (LE) coexistence, where compression of the film does not result in changes in surface pressure. As the monolayer is compressed to the point where it is in the LE phase, the surface pressure begins to rise from zero; this is denoted as the lift-off point of the isotherm. Further compression leads to a thermodynamic transition to the condensed (C) phase, during which the isotherm plateaus and the film is in a LE-C coexistence region. Upon the complete conversion of LE to C phase, the isotherm begins to rise again. The film is eventually compressed to the point where the surface area is smaller than the total cross-sectional area of the lipids, at which point the monolayer collapses with materials leaving the 2D film and exploring the third dimension. For DPPC, collapse occurs at a surface pressure of ~72 mN m⁻¹.

In order to understand the role of sugar molecular structure in lipid/sugar interactions under physiological salt concentrations, we introduced different molecules (glycerol, glucose, and trehalose) in the subphase and performed pressure–area isotherms of DPPC monolayers in the absence and presence of 100 mM NaCl. We found that as the structural complexity of the sugar increased, the amount of sugar/polyol required for a similar effect on the lipid film decreased. We first performed experiments with a moderate amount of glycerol in the subphase and found that even with up to 20% glycerol, in the absence or the presence of 100 mM NaCl, the isotherm does not exhibit much change (Figure 1). Unlike glycerol, which is a straight-chain triol, glucose forms a stable six-member ring in solution, and its inclusion in the subphase affects the phase behavior of the lipid monolayer. While 5% glucose does not have much of an effect on the isotherm, the addition of 100 mM NaCl leads to a synergistic interaction, resulting in a right shift of the isotherm. This shift can be observed from lift-off until collapse of the monolayer. The right shift in the isotherm indicates that in the presence of both glucose and NaCl the lipid molecules sense the similar effects of their neighbors but at a larger distance compared to when only water is present. Using a reduced amount of 2.5% glucose leads to insignificant changes to the isotherm even in the presence of 100 mM NaCl (data not shown).

Next, we examined the impact of trehalose on DPPC monolayers. Trehalose is a disaccharide composed of two glucose monomers and is known to alter membrane properties under freeze-drying conditions and to interact with hydrated

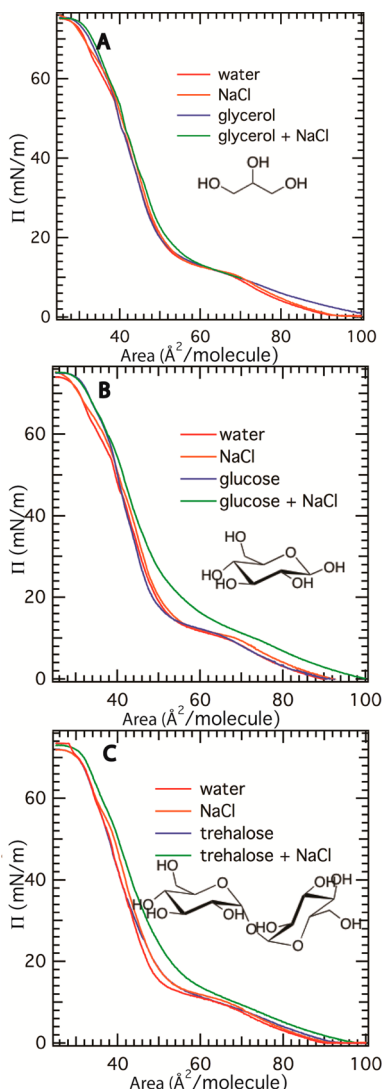


Figure 1. Pressure–area isotherms of DPPC monolayers at 25 °C in the absence and presence of 100 mM NaCl for a subphase with (A) 20% glycerol, (B) 5% glucose, and (C) 2.5% trehalose. The small kink in the high surface pressure region is due to slight creepage of the film, resulting in a lower area at collapse.

DMPC bilayers.³⁹ When 5% trehalose alone was added to the subphase, a significant shift in the isotherm was observed (data not shown). Further experiments were performed using 2.5% trehalose, which gave results similar to those obtained using 5% glucose (Figure 1C), showing a right shift of the isotherm upon the addition of 100 mM NaCl. Since the structure of the sugar clearly has a significant effect on the interactions observed in the presence of NaCl, we conclude that the observed effects rely upon specific sugar–lipid interactions.

FM and AFM Imaging: Enhanced Chirality of DPPC Domains in the Presence of Glucose. Fluorescence imaging provides micron-level resolution of the surface morphology of the monolayer. Changes to the surface morphology can provide clues as to how the subphase components are interacting with the monolayer. Figure 2 shows FM images taken at 15 mN/m for DPPC on water, 100 mM NaCl, 5% glucose, and 100 mM NaCl + 5% glucose. This surface pressure was chosen because it is in the coexistence region for all samples examined and therefore allows for direct comparison of domain structure found in the different systems. Images at higher surface

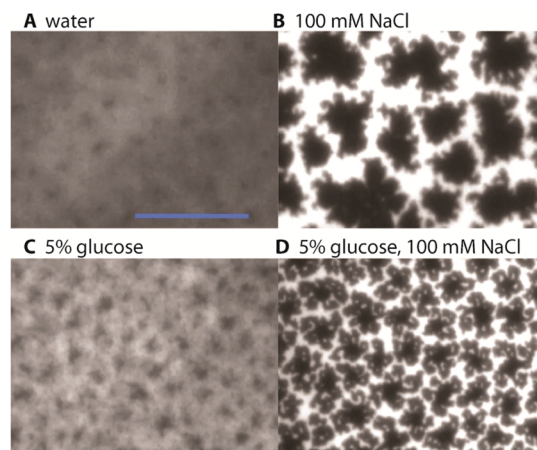


Figure 2. FM images of DPPC monolayers at 25 °C and 15 mN/m for subphase composed of (A) water, (B) 100 mM NaCl, (C) 5% glucose, and (D) 100 mM NaCl and 5% glucose. Scale bar is 100 μ m.

pressures (e.g., 30 mN m⁻¹), where all or most of the monolayer is in the condensed phase, do not clearly show the domain structure (see Supporting Information) as the condensed phase excludes the bulky Texas Red probe.

Comparison of FM image for DPPC on pure water (Figure 2A) with that of 100 mM NaCl (Figure 2B) shows that the presence of salts results in “rounder” or less branched domain shapes. Domain shapes are dictated by the combined effects of electrostatic repulsions, line tension, and spontaneous curvature due to chirality.⁴⁰ Electrostatic repulsions are reduced by the presence of 100 mM NaCl, which increases the relative importance of the line tension contribution. Increasing the line tension minimizes the length of the domain edge, leading to the observed “rounder” domain in the 100 mM NaCl subphase when compared to pure water.

Morphology of DPPC domains on pure water does not differ much from that with 5% glucose (Figure 2C). In both cases, the condensed domain shapes contain features that are below the resolution of the optical microscope and therefore are not discernible. As a result, these FM images are gray and exhibit low contrast. However, comparison of FM image for the 100 mM NaCl subphase with that for the 100 mM NaCl + 5% glucose subphase shows enhanced chiral features in the domain shape in the latter. Since the DPPC molecule is chiral, its condensed phase exhibits asymmetric domain shapes. The addition of bulky sugar molecules to the chiral headgroup acts to enhance domain shape asymmetry, leading to increased spontaneous curvature.³⁴ This interpretation is consistent with the finding that addition of trehalose to the subphase of dioleoylphosphatidylethanolamine (DOPE) monolayers increases monolayer curvature, likely due to trehalose–DOPE interactions that alter the interfacial geometry.¹⁵ Sugars binding specifically to the headgroup can increase the chirality of the domain shape³⁴ and may serve to account for the morphological changes observed in our FM images. The increased spontaneous curvature observed in FM with both sugar and salt, as opposed to with only salt present in the subphase, suggests that the sugar interact specifically with the membrane.

FM images capture different monolayer morphologies on the micron length scale. To resolve features at a higher resolution, AFM imaging was performed on each monolayer transferred from the air/liquid interface onto a solid mica support. These

micrographs show monolayer morphology with nanometer resolution in the lateral direction and angstrom resolution in the vertical direction. Each monolayer was deposited at a surface pressure of 30 mN m^{-1} . This surface pressure was chosen as it is necessary to have a relatively densely packed monolayer in order to ensure that the surface features are preserved upon transfer. Figures 3A–D show AFM images of DPPC on pure water, 100 mM NaCl, 5% glucose, and 100 mM NaCl + 5% glucose, respectively, transferred at 30 mN/m .

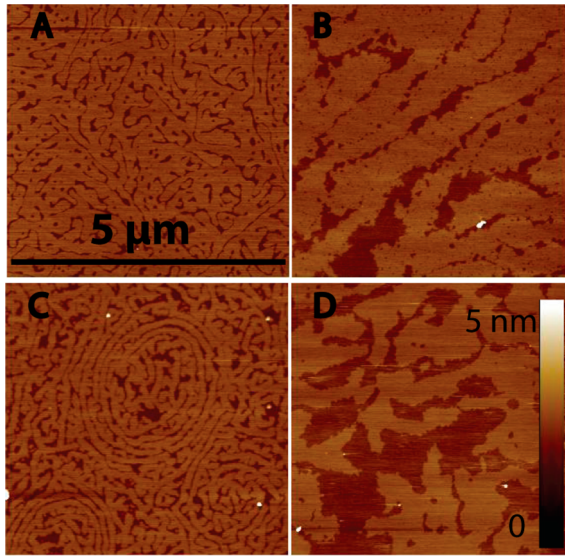


Figure 3. AFM images for DPPC monolayers on mica substrates transferred at 25°C , 30 mN/m for a subphase composed of (A) water, (B) 100 mM NaCl, (C) 5% glucose, and (D) 5% glucose and 100 mM NaCl. Scale bar is 5 nm. Lateral size of each image is 5 μm .

Lipids within the condensed domains pack with a short-range, in-plane ordered structure where the *all-trans* hydrocarbon chains are in positional registry. In the less ordered or more fluid phase, the hydrocarbon chains of lipid molecules have more space and therefore retain a greater amount of conformational freedom. When a biphasic (LE/C) DPPC monolayer is deposited onto mica, the condensed domains are $\sim 0.8 \text{ nm}$ taller than the fluid domains due to the difference in packing and tilt of the acyl chains.³³ Since all monolayers examined are phase-separated at the surface pressure of deposition, the height of numerous condensed domains can be used as a reference state. Any phase that appears lower in height than the C phase is by definition more disordered in nature.

AFM micrographs (Figure 3) show brighter condensed domains with darker (lower in height by $\sim 0.8 \text{ nm}$) regions interspersed within the domains. The height variation was determined by line scans, which are included in the Supporting Information along with corresponding histograms. Monolayers with NaCl present in the subphase contain larger patches of disordered regions than monolayers without NaCl. This effect is clear from the increased area of regions with lower heights observed in the monolayer (particularly within the condensed domains on the AFM images).³³ Furthermore, distinct increase in the chirality of the domains can be observed in the sample with 5% glucose present (Figure 3C) compared to the pure water case (Figure 3A), an effect that is not discernible from

examining their corresponding FM images in Figures 2C and 2A due to the lower resolution.

Neutron Reflectometry: Glucose and/or NaCl Reduce DPPC Headgroup Hydration. Neutron reflectometry was performed on DPPC-d75 monolayers to better understand how out-of-plane structure of the monolayer is influenced by the addition of glucose and/or NaCl. In monolayers at the air/liquid interface, these data help determine the extent to which glucose, NaCl, and water penetrate the headgroup or form a boundary layer at the headgroup/subphase interface. NR measurements with 100 mM as well as 200 mM NaCl have been performed, but the resulting scattering profiles are very similar; here we report only results from subphase containing 200 mM NaCl. As can be seen in the NR profiles in Figure 4,

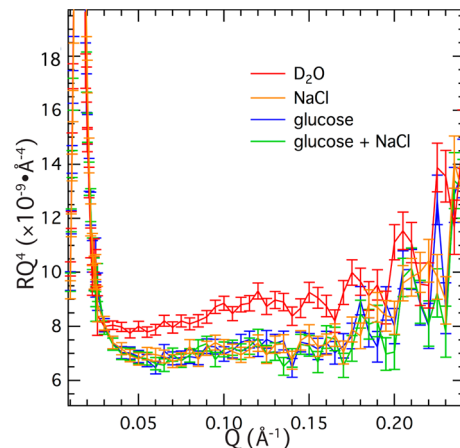


Figure 4. NR profiles for DPPC-d75 monolayers at 20 mN/m , 23°C on D_2O , with 200 mM NaCl, 5% glucose, or 5% glucose + 200 mM NaCl.

the addition of 5% glucose, 200 mM NaCl, and 5% glucose + 200 mM NaCl resulted in rather similar NR curves, which in turn were different from that obtained for a pure D_2O subphase. For simplicity, we present here comparison of only two scattering cases: DPPC-d75 on pure D_2O subphase and DPPC-d75 on D_2O containing 5% glucose (Figure 5).

Several different models were attempted to fit the data. For instance, we tried fitting by dividing the monolayer into two distinctive regions (head and tail). We also attempted to fit the lipid as a single region (head and tail together). For both the one- and two-slab models, we have further attempted to incorporate an adlayer to the lipid surface; such a fitting model might be required if particular subphase components partition near the lipid surface.² However, in the series of NR experiments described with the concentration of solutes employed, no partitioning of subphase components near the surface was observed experimentally. Further, we were unable to fit the monolayer, even in pure D_2O , to models with one or two slabs.

The NR data can only be fitted to a model in which the scattering length density distribution of the monolayer perpendicular to the liquid interface was divided into three distinctive regions (see Figure 5). In this model, the high scattering length density (SLD) for the first layer (I) represents the deuterated tail including the ester linkage, the non-deuterated second layer (II) represents the hydrogenated glycerol linker in the headgroup together with hydrating D_2O , and the third layer (III) represents the remainder of the

deuterated headgroup plus any hydrating D₂O solvent molecules.

Since the number of fitting parameters is significant, we either fixed some parameters (based on their known chemical structures) or limited their range of changes to avoid overparametrization of the problem. The three models (models 1, 2 and 3) we used to successfully fit the data are described in detail in Table S.1 in the *Supporting Information*, with all three fits shown in Figure S.1. In model 1, the fitting model with the greatest constraints, precisely measured literature values for area per molecule, tilt of the hydrocarbon tails and lipid composition were used to fix $\beta(z)$ of the tails and the thickness of tail (l_1) region.⁴¹ In addition, l_2 and l_3 were constrained based on results obtained using pure D₂O in the subphase. Also, the roughness parameters were kept in the range of 2.7–4.0 Å.³⁸ In contrast, in the case of model 3, all parameters were free. Interestingly, fitting results obtained from models 1 and 3 point to the same conclusion regarding changes in the film when glucose is present in the subphase. The raw data and fit for model 2 are shown in Figure 5. For this model, $\beta(z)$ for the layers II and III were free, while the other parameters were constrained, with roughness parameters restricted within the allowable regime.

For DPPC-d75 on the 5% glucose/D₂O subphase our models (1, 2, 3) result in similar parameters. The biggest difference between the pure D₂O and the glucose/D₂O data is in the $\beta(z)$ of region II. The theoretical (dry) $\beta(z)$ for region II is $0.9 \times 10^{-6} \text{ Å}^{-2}$. On the pure D₂O subphase region II $\beta(z)$ is $4.27 \times 10^{-6} \text{ Å}^{-2}$. When 5% glucose or 200 mM NaCl is added into the subphase, the SLD of this region decreases to $(2.52\text{--}3.88) \times 10^{-6} \text{ Å}^{-2}$, depending on which model is used. This reduction in SLD in region II may correspond to change in hydration or replacement of deuterated water with hydrogenated glucose or a combination of both. If the change in $\beta(z)$ is due entirely to hydration, the change in hydration can be calculated by

$$\beta(z)_{\text{II}} = \beta(z)_{\text{sub}}x + \beta(z)_{\text{dry}}(1 - x)$$

where $\beta(z)_{\text{II}}$ is the calculated $\beta(z)$ of layer II from the data, $\beta(z)_{\text{sub}}$ is the value for the D₂O subphase, $\beta(z)_{\text{dry}}$ is the theoretical $\beta(z)$ of layer II in the absence of any hydration, and x is the volume fraction of water present in layer II. For lipid with the pure D₂O subphase, layer II is

$$4.27 = 5.65x + 0.9(1 - x), \quad x = 0.71, \text{ or } 71\% \text{ hydrated}$$

In the case of 5% glucose in the subphase, this hydration of layer II can be as low as

$$2.52 = 5.65x + 0.9(1 - x), \quad x = 0.35, \text{ or } 35\% \text{ hydrated}$$

We do not observe a clear difference in hydration of layer III, but given the similar $\beta(z)$ of D₂O and region III, our NR measurements are less sensitive to probe hydration of region III.

Since similar NR results are seen even in the case of 200 mM NaCl with no glucose present, we favor the explanation that the difference in the NR is predominately due to changes in hydration of layer II. As shown in the calculations above, the hydration of layer II can drop from 71% on pure D₂O to 63% or as low as 35% (depending on the model) in the presence of 5% glucose. This result is consistent with the osmotic effects documented in the literature and is caused by the partial exclusion of solute from the hydration layer.⁴² While we do not

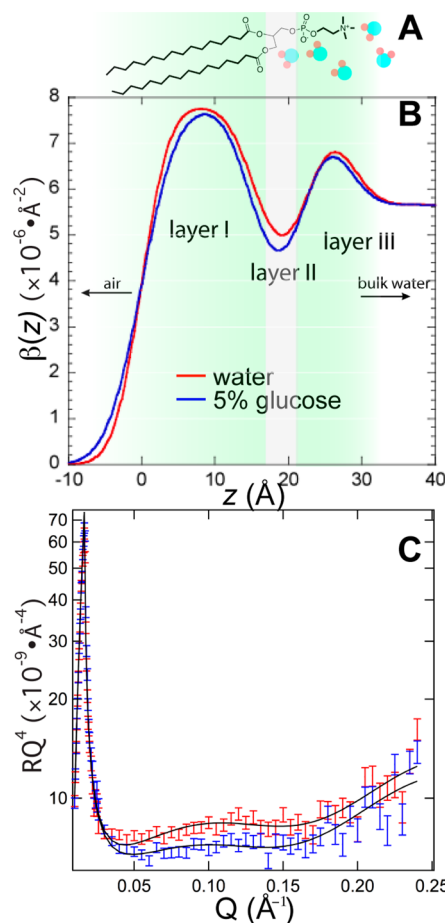


Figure 5. (A) Depiction of DPPC-d75 at the air/D₂O interface, where perdeuterated carbons are in bold. Layer I includes the deuterated fatty acid tails. Layer II includes the hydrogenated carbon atoms from the glycerol linker. Layer III includes the deuterated polar headgroup. (B) Scattering length density, $\beta(z)$, vs distance for the fit using model 2 on pure D₂O (red) and 5% glucose (blue). (C) Raw data and respective fits for the NR data on pure water (red) and 5% glucose (blue).

observe any partitioning of glucose to the lipid surface from our NR analysis at the glucose concentration used in our experiments, the imaging and isotherm pressure-area data nevertheless indicate that the presence of glucose and NaCl in the subphase leads to substantial morphological changes in the DPPC monolayer.

Role of Anions. We examined the effect of 100 mM NaF, NaCl, or NaBr on the isothermal compression of a DPPC monolayer in the absence and presence of 5% glucose or 2.5% trehalose (Figure 6). The salts by themselves had very little influence on the isotherm (Figure 6A). However, in the presence of 5% glucose or 2.5% trehalose, all of the salts have a similar, synergistic effect on the isotherm (see Figures 6B and 6C, respectively). Furthermore, FM images (see *Supporting Information*) for the various salt samples have quite similar effects in giving rise to “rounder” and less branched domains, though there are characteristics differences in terms of domain number density, domain size, and shape observed.

Further studies were performed using 200 mM NaCl with 5% glucose or 2.5% trehalose to examine the salt concentration dependence of these systems. Isotherms at 200 mM salt concentrations are provided in the *Supporting Information*, showing trends similar to those observed at 100 mM salt. To

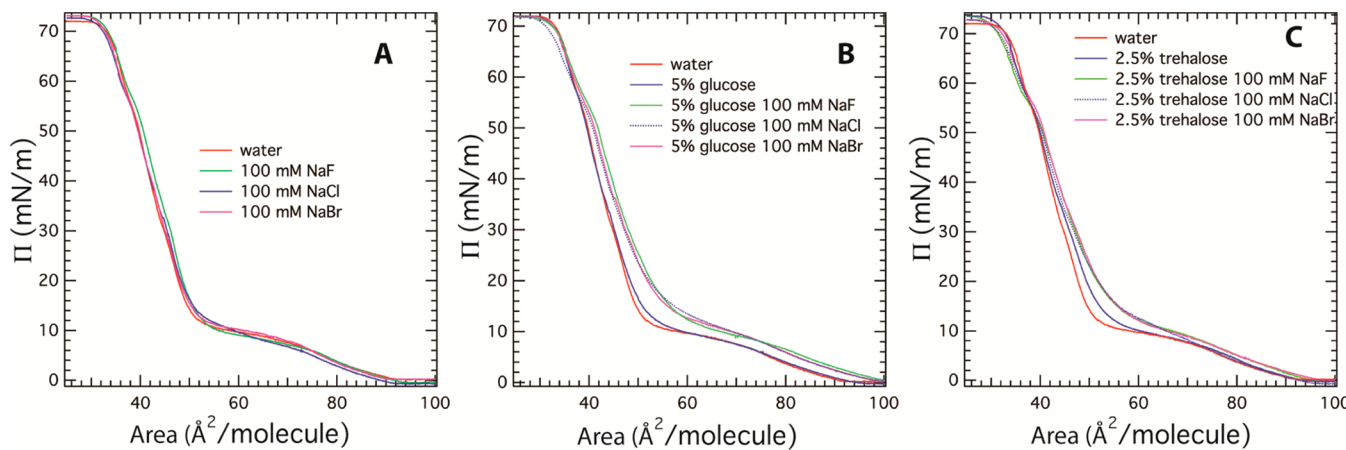


Figure 6. Isotherms on DPPC monolayers at 25 °C for (A) water, (B) 5% glucose, and (C) 2.5% trehalose, all with 100 mM of NaF, NaCl, or NaBr.

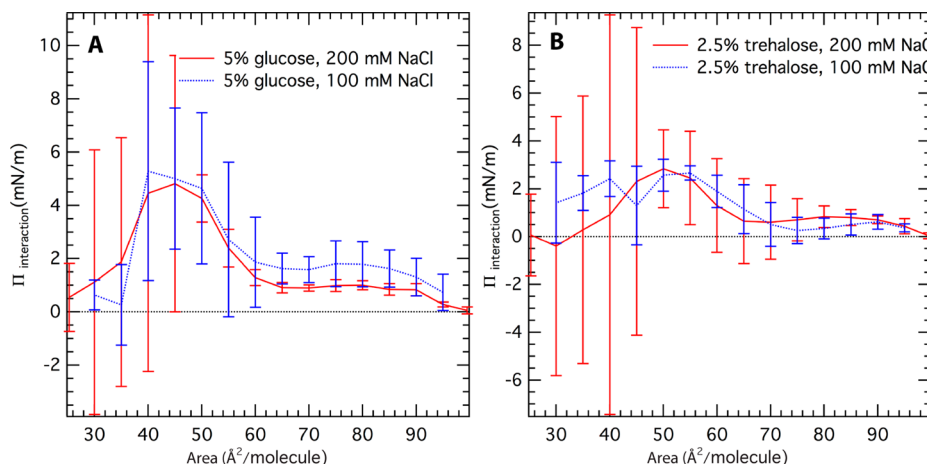


Figure 7. $\Pi_{\text{interaction}}$ values for 100 or 200 mM NaCl obtained from pressure–area isotherms on DPPC monolayers at 25 °C for subphases with (A) 5% glucose and (B) 2.5% trehalose.

to better quantify possible differences between the 100 and 200 mM NaCl subphases in the presence of sugar, we first calculated the expected surface pressure values assuming that the effects of sugar and salt on the isotherms are purely additive using the following equation:

$$\Pi_{\text{intrinsic}} = \Pi_{\text{sugar}} + \Pi_{\text{salt}} - \Pi_{\text{water}}$$

Here, Π_{sugar} is the surface pressure when only sugar is present, Π_{salt} when only salt is present, and Π_{water} when the subphase is pure water. $\Pi_{\text{intrinsic}}$ thus refers to the expected shift in the isotherm in the absence of any competing or cooperative interaction when both sugar and salt are present. Any additional shift (i.e., cooperative or competitive result) will then be captured in the term

$$\Pi_{\text{interaction}} = \Pi_{\text{sugar+salt}} - \Pi_{\text{intrinsic}}$$

where $\Pi_{\text{sugar+salt}}$ is the surface pressure when both sugar and salt are present, and a positive value for $\Pi_{\text{interaction}}$ reflects a right shift in the isotherm, indicating a larger surface pressure at a given area/molecule. Values for $\Pi_{\text{interaction}}$ were determined at intervals of 5 $\text{\AA}^2/\text{molecule}$, where raw values were averaged over $\pm 0.5 \text{\AA}^2/\text{molecule}$, and the error bars in Figure 7 represent the standard deviation obtained from three independent measurements. As indicated in Figure 7, $\Pi_{\text{interaction}}$ values are similar for the two different salt concentrations. The overall effect is greater for 5% glucose (Figure 7A) than for 2.5%

trehalose (Figure 7B), but the trends are quite similar. Differences in magnitude in $\Pi_{\text{interaction}}$ may also be accounted for by the different sugar concentrations used.

Role of Cations. In order to evaluate the role of the cation in lipid–sugar–salt interactions, we studied the effect of 100 mM LiCl, NaCl, and KCl on the isothermal compression of DPPC monolayers in the presence of 5% glucose or 2.5% trehalose. Using a salt concentration of 100 mM, our results indicate that NaCl has a greater effect on the isotherm than either LiCl or KCl (data not shown). In an attempt to enhance this effect, we further increased the salt concentration to 200 mM.

The isotherms of DPPC monolayer on 200 mM salt-only subphases (water, LiCl, NaCl, and KCl) are shown in Figure 8, with that for LiCl shifting slightly to the right relative to that for NaCl or KCl. The same trend was also observed with 100 mM salt (data not shown). This shift suggests that Li^+ , even in the absence of sugar, interacts with the membrane in a more significant manner compared to the other cations. FM images obtained at 15 mN/m (Figure 9) demonstrate that domain size is smaller for the LiCl subphase than for subphases containing NaCl or KCl.

Since the salts by themselves shift the isotherm, we could not directly compare the effect of the sugar/salt combinations. To simplify our analysis, we again determined $\Pi_{\text{interaction}}$ values at intervals of 5 $\text{\AA}^2/\text{molecule}$, where raw values were averaged

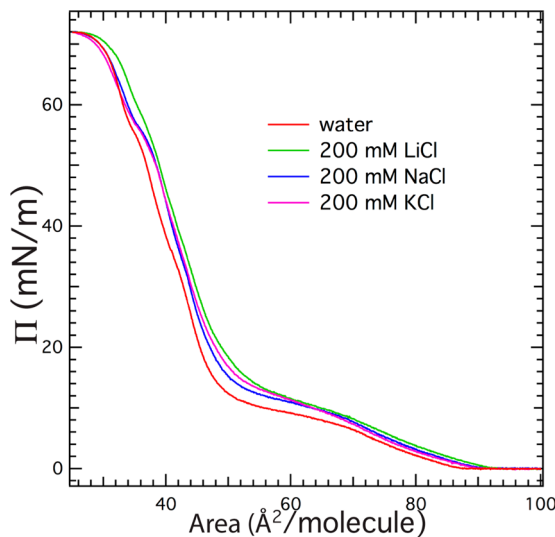


Figure 8. Isotherms of DPPC monolayers at 25 °C for water in the absence and presence of 200 mM salts (LiCl, NaCl, or KCl).

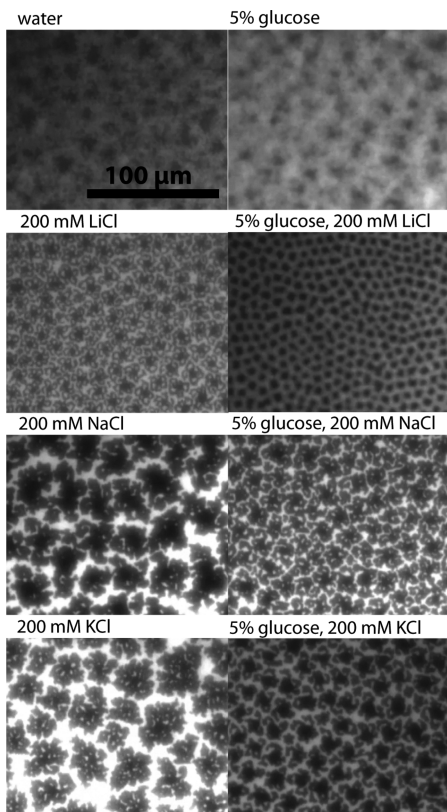


Figure 9. FM images of DPPC monolayers at 25 °C and 15 mN/m on water, 200 mM LiCl, 200 mM NaCl, 200 mM KCl, and in the absence (left) and presence (right) of 5% glucose.

over $\pm 0.5 \text{ \AA}^2/\text{molecule}$, and the error bars in Figure 10 represent the standard deviation resulting from three independent measurements. Our results, shown in Figure 10, demonstrate that NaCl gives rise to a larger $\Pi_{\text{interaction}}$ with 5% glucose than does KCl or LiCl. Similar trends, albeit to a smaller extent, are observed with 2.5% trehalose at 200 mM salt concentrations.

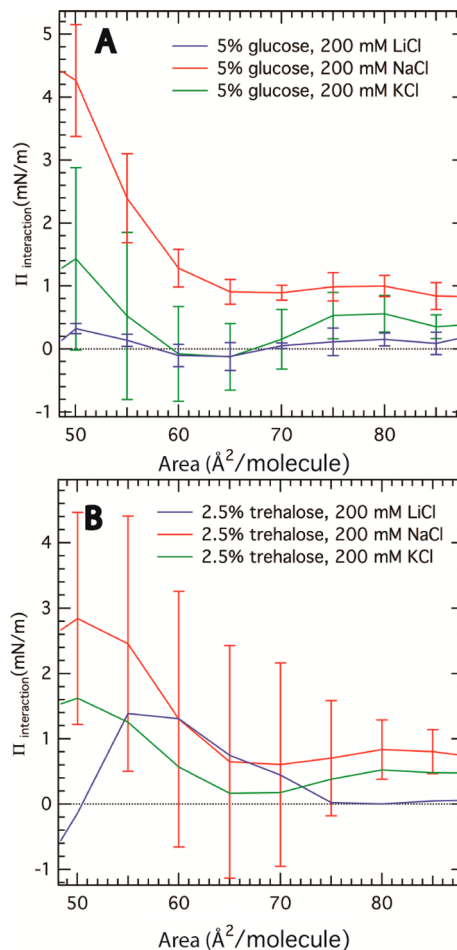


Figure 10. $\Pi_{\text{interaction}}$ values for subphases with 200 mM salts (LiCl, NaCl, or KCl) obtained from pressure-area isotherms of DPPC monolayers at 25 °C with (A) 5% glucose and (B) 2.5% trehalose.

DISCUSSION

On the basis of the results described, we conclude that while there is no significant thermodynamic driving force for glucose–lipid interactions, glucose that remains near the surface associates with the monolayer in a way that perturbs lipid morphology. Our NR results (Table S.1) did not reveal any partitioning of glucose near the lipid surface at the glucose concentrations examined, in either the presence or absence of NaCl. These results are consistent with literature suggesting that glucose may be partially excluded from zwitterionic membranes, leading to dehydration of the monolayer.^{5,14,15} Nevertheless, our AFM results demonstrate that glucose perturbs the morphology of DPPC monolayers on water (Figure 3). Similar perturbations were observed for lipid monolayers on NaCl subphase when glucose was added, as domain structures in the presence of glucose and NaCl were more chiral than when only NaCl was present (Figure 2). At first glance, the NR and imaging results may appear to be in contrast, yet they are consistent with recent reports that both glucose and trehalose interact with DMPC vesicles and are enriched at low sugar concentrations, but as sugar concentration are increased, binding sites become saturated and the sugars are excluded from the membrane.^{20,21} Therefore, sugar exclusion at the surface does not necessarily correlate with specific sugar–lipid interactions. Specific interactions are likely

taking place in our system, but variation in sugar concentrations near the surface were not detected in our NR experiments.

The observed rightward shift in the isotherms only when both glucose and NaCl were present (Figure 1) is indicative that the interaction of glucose with the membrane is increased in the presence of salt. The supposition that the observed right shift in the isotherm is caused by specific sugar–lipid interactions is supported by several reports in the literature. Cyclized polyols were found to display residual dipolar couplings consistent with membrane alignment, indicating a specific relative orientation and H-bonding pattern between the polyols and the PC headgroup.¹² The observed alignment was also dependent on the structure of the polyol, strongly supporting the likelihood of specific lipid–polyol interactions.¹² Similar studies indicated that trehalose binds to DMPC membranes in a preferred conformation, with H-bonds forming between specific hydroxyls on trehalose and the phosphoate headgroup.³⁹ Numerous modeling studies also support specific interactions of sugars at the membrane surface.^{18–21,39} Our FM images along with supporting literature suggest that glucose associates with the lipid in a specific orientation. It may be that the entropic cost of orienting the glucose molecule balances any favorable enthalpic gains, resulting in a net-zero thermodynamic gain.^{14,42} This would explain why we do not see any partitioning of glucose near the surface, yet observe significant morphological changes to the monolayer. This may also explain why lipid–sugar interactions are difficult to characterize and are sensitive to the specific system being studied. In our case, we were able to perturb interactions between glucose and a zwitterionic lipid film by simply adding NaCl.

This view of glucose–lipid interactions is consistent with others that find sugars effective at protecting membranes during freeze-drying, due in part to an osmotic effect.¹⁵ The reduced concentration of solute near the lipid surface creates an osmotic gradient, which draws additional solvent out of the membrane.⁴² However, specific sugar–lipid interactions are also thought to play an important role in protection.^{4,43} These effects are known to depend upon the sugar structure. In particular, $\alpha,\alpha,1,1$ -linkage between the two glucose subunits in trehalose is thought to provide a balance of flexibility and rigidity,¹⁷ thus allowing it to form strong interactions with multiple lipid headgroups.¹⁹ This may explain why a lower concentration of trehalose compared to glucose was required to elicit similar effects. Recent work has shed light on other mechanisms by which small molecules may impart cryoprotection, specifically water “structure-making” properties of certain reagents. For example, NMR experiments recently revealed that a significant mechanism by which DMSO offers protection is by forming strong H-bonds with water, which compete with water–lipid H-bonds, dehydrating the surface.²² Interestingly, that model is further supported by molecular dynamics simulations that highlight specific DMSO–lipid interactions,²³ illustrating how multiple mechanisms apply to the same system.

In order to understand how NaCl influences the sugar–lipid interactions, we varied separately the anion (F^- and Br^-) and cation (Li^+ and K^+) and observed changes to the isotherms and surface morphology of DPPC monolayers in the presence or absence of glucose or trehalose. By varying the anion, we sought to determine if anions compete with glucose or trehalose for lipid interaction. While anions are not expected to interact in a specific manner with the PC headgroup, Leontidis and co-workers have demonstrated that anions

partition into the LE phase of DPPC monolayers according to the Hofmeister series.⁴⁴ While fluoride is excluded from the LE phase of DPPC monolayers,⁴⁵ chloride partitioning is intermediate, and bromide partitions preferentially.⁴⁶ Since similar isotherms (Figure 6) and FM images (Figure S.3) were observed for NaF, NaCl, and NaBr, we conclude that anions do not compete with the ability of glucose or trehalose to associate with the membrane under the experimental conditions described.

Further, we sought to understand the role of cations in perturbing lipid–sugar interactions. Divalent cations such as Ca^{2+} have long been known to chelate lipid headgroups, but a number of recent studies have demonstrated that monovalent Na^+ or Li^+ is able to interact with the lipid headgroup to a greater extent than previously thought.^{47,48} Solution-phase molecular-resolution AFM studies demonstrated that $CaCl_2$ and $NaCl$ lead to similar changes in the lipid headgroup structure in DPPC bilayers in the gel phase.⁴⁹ The observed conformational changes are consistent with theoretical models that show cation binding tilts the headgroup out of the membrane plane.^{49,50} In AFM studies,⁴⁹ the level of cation–lipid interaction increases with increasing charge density following the Hofmeister series, in the order $K^+ < Na^+ \ll Ca^{2+}$. Also, theoretical frameworks have recently demonstrated that sodium and lithium ions can bind to the carbonyl and phosphate functional groups in zwitterionic lipids.⁴⁷ Few studies have examined how Li^+ interacts with lipids, but it has been shown that Li^+ binding to a palmitoyl-oleoyl-phosphatidylcholine bilayer is stronger than Na^+ but weaker than Ca^{2+} binding.⁴⁸ The rightward shift in the compression isotherms at 200 mM salt concentrations (Figure 8) is also consistent with increased Li^+ binding. Thus, on the basis of our results and a review of the literature, we conclude that K^+ binds the PC headgroup weakly, Na^+ binding is intermediate, and Li^+ binding is the strongest among the cations investigated.

It has been proposed by others that binding of cations leads to heterogeneities that allow other molecules (such as anions) to partition into the membrane.⁴⁶ We propose that the conformational change in the lipid headgroup induced by cation binding⁴⁹ may also allow carbohydrates to gain better access to the headgroup. Even though Li^+ interacts more strongly with the membrane, Na^+ results in the largest values for $\Pi_{interaction}$ with both 5% glucose and 2.5% trehalose (Figure 10). This can be explained by considering that competitive and cooperative interaction channels may exist. The fact that 200 mM LiCl by itself results in a significant shift in the isotherm suggests that Li^+ occupies many of the available binding sites. While Li^+ binding creates heterogeneity, its strong binding capability also means that it would compete with the sugars for access to the lipid headgroup region. Sodium binding strength is only intermediate and can thus induce heterogeneity without competing with glucose for association sites. On the other hand, K^+ has a low charge density, so it does not readily chelate carbonyls or phosphates, and is too large to easily penetrate into the lipid headgroup.⁴⁷ Thus, KCl has very little effect on the membrane or on glucose binding.

CONCLUSIONS

Elucidation of the mechanism of sugar–lipid interactions is important for our understanding of numerous biological phenomena, such as the protection from freezing that sugar imparts on plants and the loss of lung compliance in diabetic patients. We have found in our study that, in addition to an

osmotic effect, sugars interact specifically with lipid monolayers, leading to distinct morphological changes. These changes are influenced by the addition of monovalent salts, though salts alone have only subtle effects on the monolayer under the described conditions. Together our isotherm, FM and AFM data show that sugars interact specifically with the membrane, resulting in significant morphological changes. However, NR demonstrates that very little (if any) sugar partitions to the surface. This suggests that the interaction between sugar and lipid has a weak driving force at room temperature but nevertheless leads to significant structural perturbations of the film. Importantly, the observed effects do not exactly follow the Hofmeister series and are found to be greatest for Na^+ , suggesting that both cooperative and competing effects need to be considered.

■ ASSOCIATED CONTENT

§ Supporting Information

The Supporting Information is available free of charge on the ACS Publications website at DOI: [10.1021/acs.langmuir.5b02815](https://doi.org/10.1021/acs.langmuir.5b02815).

Abbreviations, detailed methods, NR fitting parameters and fits, AFM line scans, and supporting FM images and isothermal compressions ([PDF](#))

■ AUTHOR INFORMATION

Corresponding Author

*Ph (773) 702-7068; Fax (773) 702-0805; e-mail kayeelee@uchicago.edu (K.Y.C.L.).

Present Address

G.A.C.: Department of Chemistry, University of Illinois, Chicago, Chicago, IL.

Notes

The authors declare no competing financial interest.

■ ACKNOWLEDGMENTS

We thank Dr. Sushil Satija for help and advice during the neutron scattering experiments. This work was supported by the National Science Foundation through Grant MCB-1413613 and the NSF-supported MRSEC program at the University of Chicago (DMR-1420709). The Manuel Lujan Jr. Neutron Scattering Center at LANSCE is funded by the DOE Office of Basic Energy Sciences at Los Alamos National Laboratory under DOE Contract AC52-06NA25396.

■ REFERENCES

- (1) Holm, B. A.; Venkitaraman, A. R.; Enhorning, G.; Notter, R. H. Biophysical inhibition of synthetic lung surfactants. *Chem. Phys. Lipids* **1990**, *52*, 243–250.
- (2) Pocivaysek, L.; Gavrilov, K.; Cao, K. D.; Chi, E. Y.; Li, D. X.; Lin, B. H.; Meron, M.; Majewski, J.; Lee, K. Y. C. Glycerol-Induced Membrane Stiffening: The Role of Viscous Fluid Adlayers. *Biophys. J.* **2011**, *101*, 118–127.
- (3) Sugimachi, K.; Roach, K. L.; Rhoads, D. B.; Tompkins, R. G.; Toner, M. Nonmetabolizable glucose compounds impart cryotolerance to primary rat hepatocytes. *Tissue Eng.* **2006**, *12*, 579–588.
- (4) Jain, P.; Sen, S.; Risbud, S. H. Effect of glass-forming biopreservatives on head group rotational dynamics in freeze-dried phospholipid bilayers: A ^{31}P NMR study. *J. Chem. Phys.* **2009**, *131*, 25102.
- (5) Lenne, T.; Garvey, C. J.; Koster, K. L.; Bryant, G. Effects of Sugars on Lipid Bilayers during Dehydration - SAXS/WAXS Measurements and Quantitative Model. *J. Phys. Chem. B* **2009**, *113*, 2486–2491.
- (6) Berendsen, T. A. Supercooling enables long-term transplantation survival following 4 days of liver preservation. *Nat. Med.* **2014**, *20*, 790–793.
- (7) Cypel, M.; Yeung, J. C.; Liu, M.; Anraku, M.; Chen, F.; Karolak, W.; Sato, M.; Laratta, J.; Azad, S.; Madonik, M.; Chow, C.-W.; Chaparro, C.; Hutcheon, M.; Singer, L. G.; Slutsky, A. S.; Yasufuku, K.; de Perrot, M.; Pierre, A. F.; Waddell, T. K.; Keshavjee, S. Normothermic Ex Vivo Lung Perfusion in Clinical Lung Transplantation. *N. Engl. J. Med.* **2011**, *364*, 1431–1440.
- (8) De Prost, N.; Saumon, G. Glucose transport in the lung and its role in liquid movement. *Respir. Physiol. Neurobiol.* **2007**, *159*, 331–337.
- (9) Saumon, G.; Martet, G. Effect of changes in paracellular permeability on airspace liquid clearance: Role of glucose transport. *Am. J. Physiol. Lung Cell. Mol. Physiol.* **1996**, *270*, L191–L198.
- (10) Foster, D. J.; Ravikumar, P.; Bellotto, D. J.; Unger, R. H.; Hsia, C. C. W. Fatty diabetic lung: altered alveolar structure and surfactant protein expression. *Am. J. Physiol-Lung Cell. Mol. Physiol.* **2010**, *298*, L392–L403.
- (11) Inselman, L. S.; Chander, A.; Spitzer, A. R. Diminished lung compliance and elevated surfactant lipids and proteins in nutritionally obese young rats. *Lung* **2004**, *182*, 101–117.
- (12) Fischer, D.; Geyer, A. NMR spectroscopic characterization of the membrane affinity of polyols. *Magn. Reson. Chem.* **2005**, *43*, 893–901.
- (13) Golovina, E. A.; Golovin, A.; Hoekstra, F. A.; Faller, R. Water replacement hypothesis in atomic details: effect of trehalose on the structure of single dehydrated POPC bilayers. *Langmuir* **2010**, *26*, 11118–11126.
- (14) Westh, P. Glucose, sucrose and trehalose are partially excluded from the interface of hydrated DMPC bilayers. *Phys. Chem. Chem. Phys.* **2008**, *10*, 4110–4112.
- (15) Giordano, M.; Di Gregorio, G. M.; Mariani, P. Rigidity and spontaneous curvature of lipidic monolayers in the presence of trehalose: a measurement in the DOPE inverted hexagonal phase. *Eur. Biophys. J.* **2005**, *34*, 67–81.
- (16) Kent, B.; Garvey, C. J.; Lenne, T.; Porcar, L.; Garamus, V. M.; Bryant, G. Measurement of glucose exclusion from the fully hydrated DOPE inverse hexagonal phase. *Soft Matter* **2010**, *6*, 1197–1202.
- (17) Cordone, L.; Cottone, G.; Giuffrida, S. Role of residual water hydrogen bonding in sugar/water/biomolecule systems: a possible explanation for trehalose peculiarity. *J. Phys.: Condens. Matter* **2007**, *19*, 205110.
- (18) Leekumjorn, S.; Sum, A. K. Molecular Dynamics Study on the Stabilization of Dehydrated Lipid Bilayers with Glucose and Trehalose. *J. Phys. Chem. B* **2008**, *112*, 10732–10740.
- (19) Sum, A. K.; Faller, R.; de Pablo, J. J. Molecular simulation study of phospholipid bilayers and insights of the interactions with disaccharides. *Biophys. J.* **2003**, *85*, 2830–2844.
- (20) Andersen, H. D.; Wang, C. H.; Arleth, L.; Peters, G. H.; Westh, P. Reconciliation of opposing views on membrane-sugar interactions. *Proc. Natl. Acad. Sci. U. S. A.* **2011**, *108*, 1874–1878.
- (21) Kapla, J.; Wohlert, J.; Stevensson, B.; Engstrom, O.; Widmalm, G.; Maliniak, A. Molecular Dynamics Simulations of Membrane-Sugar Interactions. *J. Phys. Chem. B* **2013**, *117*, 6667–6673.
- (22) Cheng, C. Y.; Song, J. S.; Pas, J.; Meijer, L. H. H.; Han, S. G. DMSO Induces Dehydration near Lipid Membrane Surfaces. *Biophys. J.* **2015**, *109*, 330–339.
- (23) Dabkowska, A. P.; Collins, L. E.; Barlow, D. J.; Barker, R.; McLain, S. E.; Lawrence, M. J.; Lorenz, C. D. Modulation of Dipalmitoylphosphatidylcholine Monolayers by Dimethyl Sulfoxide. *Langmuir* **2014**, *30*, 8803–8811.
- (24) Wolfe, J.; Bryant, G. Freezing, drying, and/or vitrification of membrane-solute-water systems. *Cryobiology* **1999**, *39*, 103–129.
- (25) Mazzobre, M. F.; Buera, M. D. Combined effects of trehalose and cations on the thermal resistance of beta-galactosidase in freeze-dried systems. *Biochim. Biophys. Acta, Gen. Subj.* **1999**, *1473*, 337–344.

- (26) Mazzobre, M. F.; Longinotti, M. P.; Corti, H. R.; Buera, M. P. Effect of salts on the properties of aqueous sugar systems, in relation to biomaterial stabilization. 1. Water sorption behavior and ice crystallization/melting. *Cryobiology* **2001**, *43*, 199–210.
- (27) Ohtake, S.; Schebor, C.; Palecek, S. P.; de Pablo, J. J. Effect of pH, counter ion, and phosphate concentration on the glass transition temperature of freeze-dried sugar-phosphate mixtures. *Pharm. Res.* **2004**, *21*, 1615–1621.
- (28) Ohtake, S.; Schebor, C.; Palecek, S. P.; de Pablo, J. J. Effect of sugar-phosphate mixtures on the stability of DPPC membranes in dehydrated systems. *Cryobiology* **2004**, *48*, 81–89.
- (29) Ragoonanan, V.; Wiedmann, T.; Aksan, A. Characterization of the Effect of NaCl and Trehalose on the Thermotropic Hysteresis of DOPC Lipids during Freeze/Thaw. *J. Phys. Chem. B* **2010**, *114*, 16752–16758.
- (30) Collins, K. D. Charge density-dependent strength of hydration and biological structure. *Biophys. J.* **1997**, *72*, 65–76.
- (31) Gurau, M. C.; Lim, S. M.; Castellana, E. T.; Albertorio, F.; Kataoka, S.; Cremer, P. S. On the mechanism of the Hofmeister effect. *J. Am. Chem. Soc.* **2004**, *126*, 10522–10523.
- (32) Lo Nostro, P.; Ninham, B. W. Hofmeister Phenomena: An Update on Ion Specificity in Biology. *Chem. Rev.* **2012**, *112*, 2286–2322.
- (33) Frey, S. L.; Chi, E. Y.; Arratia, C.; Majewski, J.; Kjaer, K.; Lee, K. Y. C. Condensing and fluidizing effects of ganglioside G(M1) on phospholipid films. *Biophys. J.* **2008**, *94*, 3047–3064.
- (34) Kane, S. A.; Compton, M.; Wilder, N. Interactions determining the growth of chiral domains in phospholipid monolayers: Experimental results and comparison with theory. *Langmuir* **2000**, *16*, 8447–8455.
- (35) McConnell, H. M. Structures and Transitions in Lipid Monolayers at the Air-Water Interface. *Annu. Rev. Phys. Chem.* **1991**, *42*, 171–195.
- (36) Gopal, A.; Lee, K. Y. C. Morphology and Collapse Transitions in Binary Phospholipid Monolayers. *J. Phys. Chem. B* **2001**, *105*, 10348–10354.
- (37) Pocivavsek, L.; Frey, S. L.; Krishan, K.; Gavrilov, K.; Ruchala, P.; Waring, A. J.; Walther, F. J.; Dennin, M.; Witten, T. A.; Lee, K. Y. C. Lateral stress relaxation and collapse in lipid monolayers. *Soft Matter* **2008**, *4*, 2019–2029.
- (38) Nelson, A. Co-refinement of multiple-contrast neutron/X-ray reflectivity data using MOTOFIT. *J. Appl. Crystallogr.* **2006**, *39*, 273–276.
- (39) Kapla, J.; Engstrom, O.; Stevensson, B.; Wohlert, J.; Widmalm, G.; Maliniak, A. Molecular dynamics simulations and NMR spectroscopy studies of trehalose-lipid bilayer systems. *Phys. Chem. Chem. Phys.* **2015**, *17*, 22438–22447.
- (40) Kruger, P.; Losche, M. Molecular chirality and domain shapes in lipid monolayers on aqueous surfaces. *Phys. Rev. E: Stat. Phys., Plasmas, Fluids, Relat. Interdiscip. Top.* **2000**, *62*, 7031–7043.
- (41) Brumm, T.; Naumann, C.; Sackmann, E.; Rennie, A. R.; Thomas, R. K.; Kanellas, D.; Penfold, J.; Bayerl, T. M. Conformational Changes of the Lecithin Headgroup in Monolayers at the Air/Water Interface - a Neutron Reflection Study. *Eur. Biophys. J.* **1994**, *23*, 289–295.
- (42) Westh, P. Experimental approaches to membrane thermodynamics. *Soft Matter* **2009**, *5* (17), 3249–3257.
- (43) Di Gregorio, G. M.; Ferraris, P.; Mariani, P. Wetting properties of dioleoyl-phosphatidyl-choline bilayers in the presence of trehalose: an X-ray diffraction study. *Chem. Phys. Lipids* **2010**, *163*, 601–606.
- (44) Aroti, A.; Leontidis, E.; Maltseva, E.; Brezesinski, G. Effects of Hofmeister anions on DPPC Langmuir monolayers at the air-water interface. *J. Phys. Chem. B* **2004**, *108*, 15238–15245.
- (45) Leontidis, E.; Aroti, A.; Belloni, L. Liquid Expanded Monolayers of Lipids As Model Systems to Understand the Anionic Hofmeister Series: 1. A Tale of Models. *J. Phys. Chem. B* **2009**, *113*, 1447–1459.
- (46) Leontidis, E.; Aroti, A. Liquid Expanded Monolayers of Lipids As Model Systems to Understand the Anionic Hofmeister Series: 2.
- Ion Partitioning Is Mostly a Matter of Size. *J. Phys. Chem. B* **2009**, *113* (5), 1460–1467.
- (47) Cordomi, A.; Edholm, O.; Perez, J. J. Effect of ions on a dipalmitoyl phosphatidylcholine bilayer. A molecular dynamics simulation study. *J. Phys. Chem. B* **2008**, *112* (5), 1397–1408.
- (48) Roux, M.; Bloom, M. Ca²⁺, Mg²⁺, Li⁺, Na⁺, and K⁺ Distributions in the headgroup region of binary membranes of phosphatidylcholine and phosphatidylserine as seen by deuterium NMR DI. *Biochemistry* **1990**, *29*, 7077–7089.
- (49) Ferber, U. M.; Kaggwa, G.; Jarvis, S. P. Direct imaging of salt effects on lipid bilayer ordering at sub-molecular resolution. *Eur. Biophys. J.* **2011**, *40*, 329–338.
- (50) Sachs, J. N.; Nanda, H.; Petrache, H. I.; Woolf, T. B. Changes in phosphatidylcholine headgroup tilt and water order induced by monovalent salts: Molecular dynamics simulations. *Biophys. J.* **2004**, *86*, 3772–3782.